Effect of Inclined Self-tapping Screws Connecting Laminated Veneer Lumber on the Shear Resistance

Feibin Wang,[a,#] Xinmeng Wang,[b,#] Weizhen Cai,[b,#] Cheng Chang,[b] and Zeli Que [b,*]

The load-bearing capacity and bearing stiffness formula of pin connectors in the current standard Eurocode 5 does not consider the influence of the angle on the single shear connection, especially for inclined screws connecting laminated veneer lumber (LVL). Therefore, research was conducted into the influence of the angle and friction on the load-bearing capacity and bearing stiffness of self-tapping screws connecting LVL made from Douglas fir. This study analyzed the existing calculation model of bearing capacity and stiffness and then derived a model with friction. The results showed that the load-bearing capacity and bearing stiffness in the tensile-shear mode was better than in the compression-shear mode, and that it was better with a 45° to 60° self-tapping screw angle. The lateral support can remarkably improve the bearing capacity and bearing stiffness in the compression-shear mode. The theoretical calculation formula for self-tapping screws connecting solid wood can better reflect the bearing capacity of inclined screws connecting LVL in the tensile-shear stress mode after increasing the fitting coefficient to 1.25. The safety factor was approximately 0.97 to 1.19. The proposed models in this paper are suitable for situations with friction in the compression-shear mode.

Keywords: LVL; Inclined screw; Load-bearing capacity; Stiffness; Theory formula

*Contact information: a: College of Landscape Architecture, Nanjing Forestry University, Nanjing 210037, Jiangsu, China; b: Department of Wooden Structure Construction Engineering, Nanjing Forestry University, Nanjing 210037, Jiangsu, China; *Corresponding author: zelique@njfu.edu.cn; [#]These authors contributed equally to this work and should be considered co-first authors*

INTRODUCTION

Laminated veneer lumber (LVL) is one of the most popular structural composite materials. Many scholars have done extensive research on LVL to characterize its mechanical properties produced from different tree species with formaldehyde and polyvinyl acetate (PVAC base) (Ozarska 1999; Wang and Dai 2005; Shukla and Kamdem 2008; Bal and Bektaş 2012), as well as to evaluate the suitability of some adhesives for LVL (Shukla and Kamdem 2009; Sulaiman *et al*. 2009; Adachi *et al*. 2010). At the same time, extensive experiments have been done to determine various mechanical properties of LVL, such as the bending property (Burdurlu *et al*. 2007; Sulaiman *et al*. 2009; Kılıç 2011; Bal and Bektaş 2012), adhesion property (Bal and Bektaş 2012), withdrawal capacity of nails and bolts (Shukla and Kamdem 2009; Adachi *et al*. 2010; Bal 2014), comprehensive strength (Celebi and Kilic 2007; Gaff and Gašparík 2015), with round holes, with and without reinforcement (Zhang *et al.* 2018), and more. Many studies have confirmed that LVL has a superior performance to solid wood (Özçifçi 2009; Bal *et al*. 2013; Bal 2014). Because of its high load-carrying capacity and mechanical properties, it has been used for many years as a high-performance structural material.

Screws are a popular form of connector. Self-tapping screws have the advantages of not requiring pre-drilling, they cause little damage to members, and they have stable support with less rebound, high construction efficiency, and good fire resistance performance (Audebert *et al.* 2012). In Europe and Japan, self-tapping screws have become one of the preferred fasteners for cross laminated timber connections (Hossain *et al.* 2015). At the same time, to achieve a higher load-carrying capacity and enhance the joint, the screw entry angle should not be perpendicular to the wood longitudinal direction, but inclined between 40° and 75° (Tomasi *et al.* 2010) (Fig. 1).

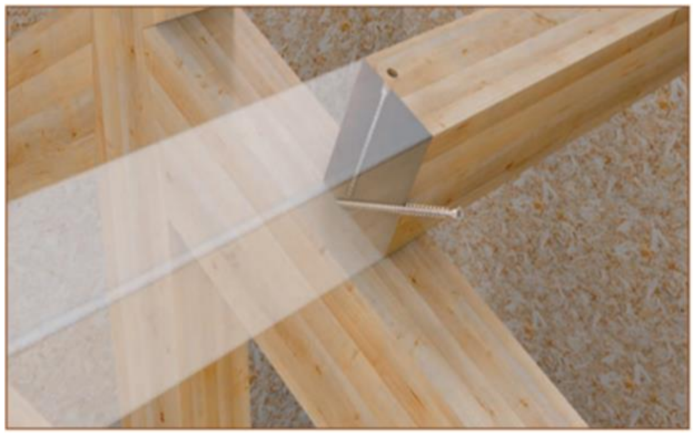

Fig. 1. Inclined self-tapping screws

In general, when using metal fasteners, such as self-tapping screws placed perpendicularly with respect to the shear plane and loaded perpendicularly to their axis, the load-bearing capacity can be calculated using the yielding theory from Johansen (1949). A large number of experimental data have been confirmed abroad, comparing the straight screw connections. In general, the load-bearing capacity of the inclined screw connection is not only derived from the bending yield strength and the withdrawal capacity of the screw, embedment strength of the timber element, but also the friction between the timber elements induced by the geometric configuration. This study explored the influence of different entry angles of self-tapping screws on LVL connections (Tomasi *et al.* 2010; Ellingsbo and Malo 2012).

EXPERIMENTAL

Materials

The LVL was made from Douglas fir (*Pseudotsuga menziesii*) in the United States and glued with a phenolic resin adhesive. Its total thickness was 43 mm, and the number of layers was 13. The thickness of an average layer was about 3.8 mm. The density was 560 kg/m^3, and the moisture content was 7.8%. Other mechanical properties of the LVL are presented in Table 1. The main and side members had the same size, and the length × width × thickness dimensions were 225 mm × 100 mm × 43 mm, respectively.

Table 1. Material Properties of LVL

Shear Modulus of Elasticity (MPa)	Modulus of Elasticity (GPa)	Compression Perpendicular to Grain (MPa)	Tensile Strength Perpendicular to Grain (MPa)	Horizontal Shear Parallel to Grain (MPa)
862.07	13.79	5.17	0.83	7.34

The self-tapping screw model was VGZ 5X100 (Rothoblaas, Cortaccia, Italy), and it is shown in Fig. 2. Its main geometric features are given in Table 2. The minimum nail margin and nail pitch of the specimens met the requirements of Eurocode 5 (EC5) (EN 1995-1-1 2008; EN 12512 2001; EN 26891 1991).

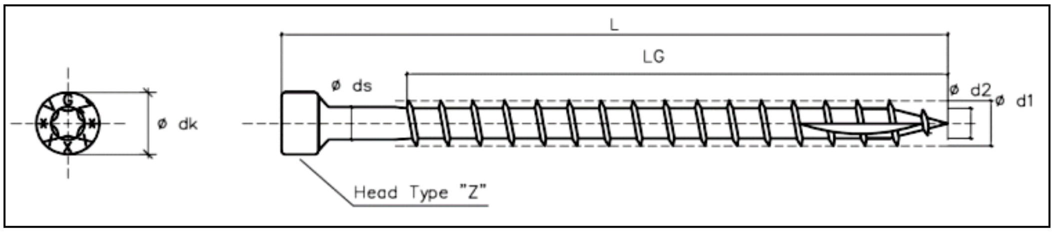

Fig. 2. Self-tapping screw model (VGZ 5X100mm)

Table 2. Main Geometric Features of the Screws

Outer Thread Diameter - d_1 (mm)	Head Diameter - d_k (mm)	Tip Diameter - d_2 (mm)	Shank Diameter - d_s (mm)	Pre-bored Hole Diameter - d_y (mm)	Full Length - L (mm)	Thread Length - b (mm)
5.3	8.0	3.6	3.95	3.0	100	90

There were two sets of specimens employed according to whether friction was applied. One set was tested without support (without friction) (Fig. 3a), and the other was tested with support (with friction) (Fig. 3b).

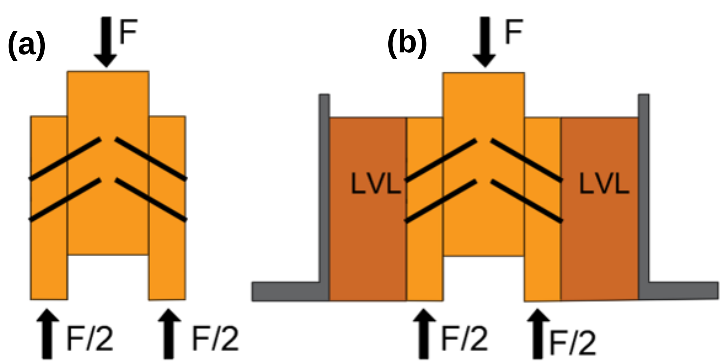

Fig. 3. Model of the specimens tested without (a) and with support (b)

The variable in each set of specimens was the angle of the self-tapping screws in the LVL components. According to the different force modes, there were two types: tensile-shear (T-S) and compression-shear (C-S); there were seven force groups: 45° C-S, 60° C-S, 75° C-S, 90° shear (S), 45° T-S, 60° T-S, and 75° T-S (Fig. 4). The loading forms of all of the specimens are shown in Fig. 3. The number of replicates per group was six.

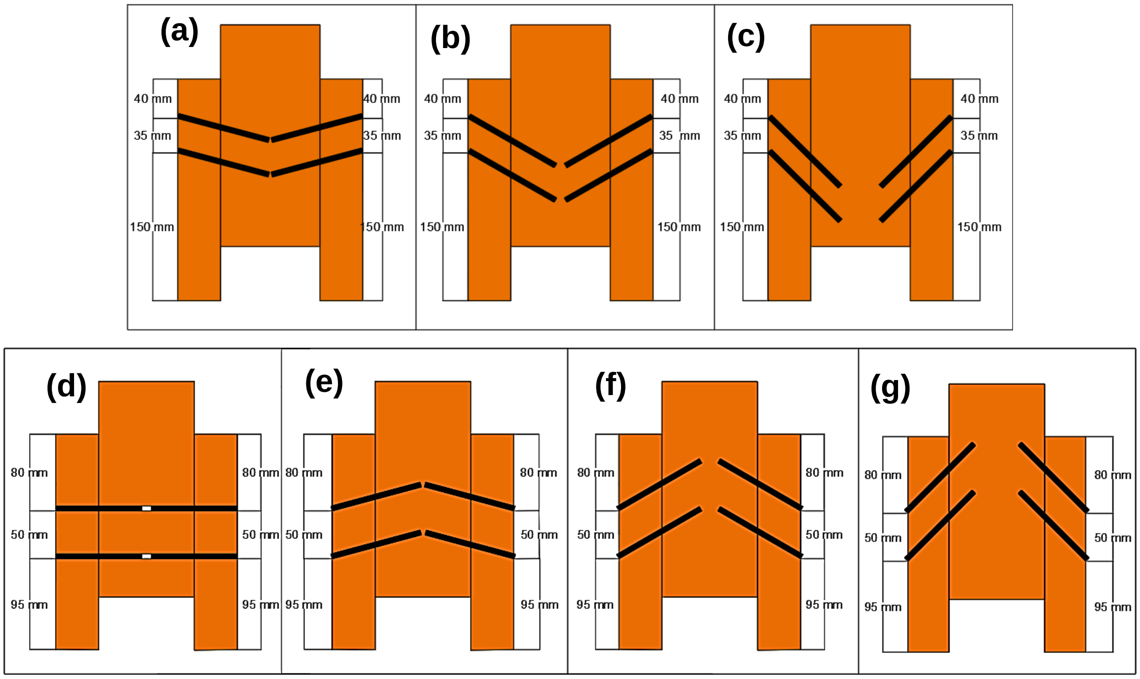

Fig. 4. Model of the LVL-to-LVL joints made using inclined self-tapping screws: 75° T-S (a), 60° T-S (b), 45° T-S (c), 90° S (d), 75° C-S (e), 60° C-S (f), and 45° C-S (g)

Methodology

The testing device used was a UTM5105 electric universal testing machine (Shenzhen Suns Technology Stock Co., Ltd., Shenzhen, China). The static monotonic was performed according to EC5 (EN 1995-1-1 2008) and LY/T 2377-2014 (2014), which determined the load-bearing capacity and stiffness. The calculation of the average value of the stiffness was according to Eqs. 1 and 2 in European Standard EN 26891 (1991).

$$k_{\mathrm{ser}} = \frac{0.4F_{\mathrm{est}} - 0.1F_{\mathrm{est}}}{v_{0.4} - v_{0.1}} \tag{1}$$

$$\begin{cases} F_{est} = mean\left(F_{max,1}; F_{max,2}; \ldots; F_{max,N}\right) \\ 0.8 \cdot F_{max,i} \leq F_{est} \leq 1.2 \cdot F_{max,i} \end{cases} \tag{2}$$

where k_{ser} is the sliding modulus (N/mm), $v_{0.1}$ is the displacement value at 0.1 times the maximum load (mm), $v_{0.4}$ is the displacement value at 0.4 times the maximum load (mm), and F_{est} is the average of all of the maximum load values (N). If, during the execution of the tests, the mean value of the maximum load of the tests already carried out deviates by more than 20 % from the estimated value, F_{est}, then F_{est} should be adjusted correspondingly for subsequent tests, which are the provisions in the standard EN 26891 (1991).

During testing, loading occurred at a uniform speed of 2 mm/min. The loads acting on the specimens were measured using a load cell that was placed between the jack and specimen. The test was stopped when the bearing capacity fell to 80% of the maximum bearing capacity. Displacement gauges were placed on both sides of the side material. The data was acquired from the control panel and TDS 530 transducers (Institute of Measuring Instruments, Tokyo, Japan) *via* a multichannel measurement device. Two series of test loading diagrams are shown in Fig. 5. Six valid specimens were tested for each configuration, and the average of the results was reported.

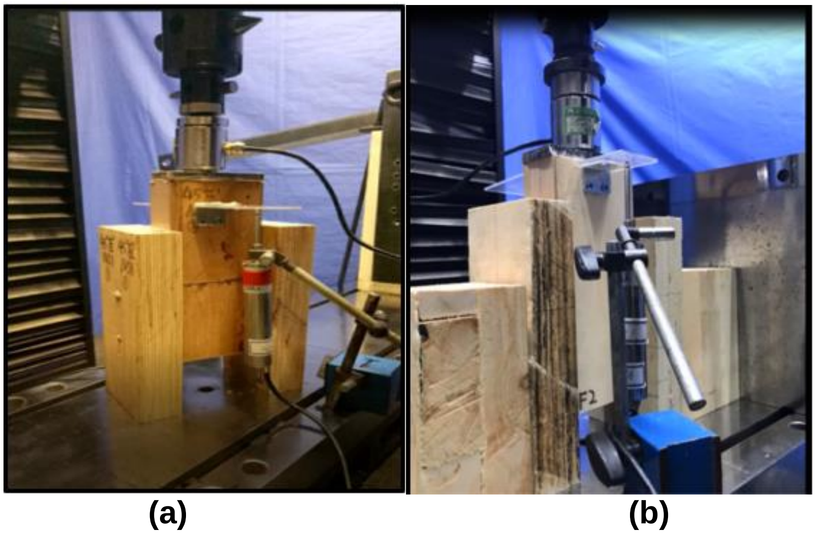

Fig. 5. Sample without (a) and with support (b) and feature of the testing machine

RESULTS AND DISCUSSION

The load-deflection curves for each configuration are shown in Fig. 6, where each curve is the average of six specimens. For the non-lateral support condition, the specimens had a better bearing performance in the T-S force mode than the C-S force mode (Fig. 6a). The lateral support obviously improved the bearing capacity of the inclined screw connecting the LVL member in the C-S force mode, and the lateral support increased the bearing capacity as the angle became smaller (Fig. 6b). However, there were two peaks when the self-tapping screws were nailed into the specimens at 75° C-S.

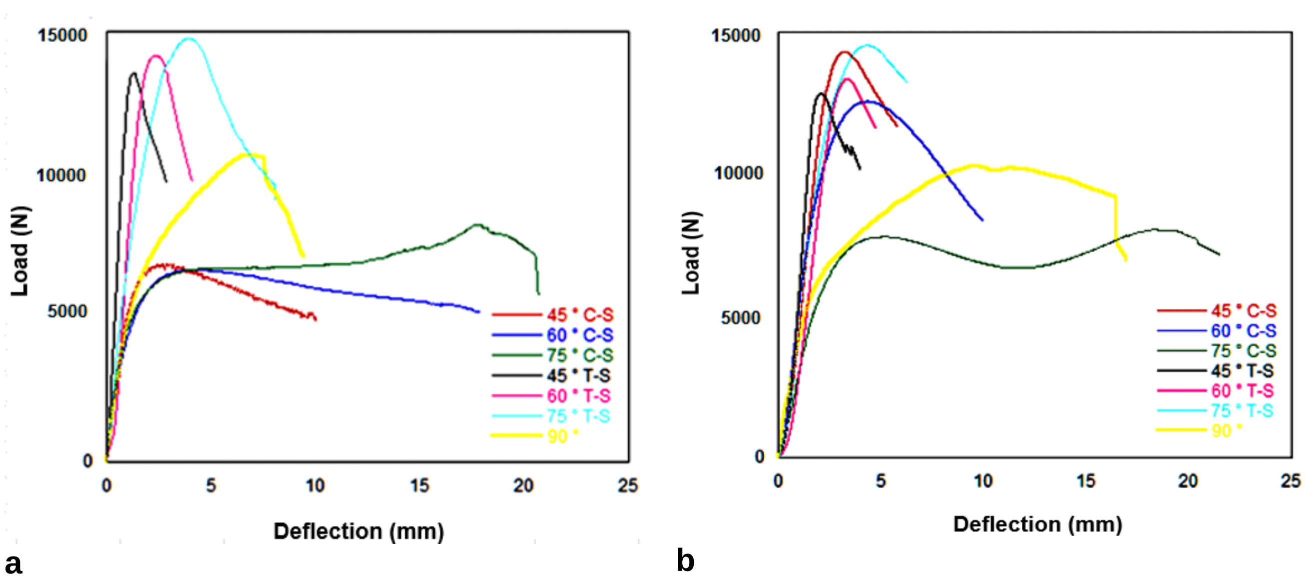

Fig. 6. Load-deflection curve of each screw angle without (a) and with support (b)

Table 3. Load-bearing Capacity and Stiffness of the Configurations

Configuration	45° T-S	60° T-S	75° T-S	90° S	75° C-S	60° C-S	45° C-S
Load-bearing Capacity (N)	13913 (13722)	14732 (14376)	14358 (14720)	10774 (10638)	7687 (8853)	7771 (12090)	8053 (14609)
Stiffness (N/mm)	14588 (15145)	9828 (9375)	6226 (6424)	3814 (3508)	2150 (2888)	5112 (6692)	6570 (7666)
The results of the tests with support are given in parentheses; the results of the tests without support are given without parentheses.							

The load-bearing capacity and stiffness results from the tests are shown in Table 3. When in the T-S mode, the lateral support had little effect on the load-bearing capacity of the joint subjected to the C-S mode. The maximum load capacities at the 75°, 60°, and 45° screw angles were 136%, 136%, and 129% of that at 90°, respectively. During the T-S process, a screw withdrawal capacity was generated because of the intertwining of the fibers and threads, so the maximum bearing capacity of the inclined screw connecting the LVL was higher than when the screw angle was 90°. The load-bearing capacity of the specimen without support in the C-S stress mode was lower than that at 90°, and the maximum bearing capacities at 75°, 60°, and 45° were 71%, 72%, and 75% of that at 90°, respectively. When the force mode was connected, the main and auxiliary materials tended to separate, and the friction disappeared, thereby further reducing the load-bearing capacity. The bearing capacity of the specimens with support in the C-S mode was obviously improved compared with the specimens without lateral support because the lateral support ensured the sustained action of friction, and the bearing capacity increased as the angle became smaller. The maximum bearing capacities at 75°, 60°, and 45° were 83%, 114%, and 137% of that at 90°, respectively, compared with the test group without support, and the bearing capacity increased by 13%, 36%, and 45%, respectively.

When in the T-S mode, there was little effect on the stiffness with or without support. Over the interval of 90° to 45°, the stiffness of the joint increased obviously as the angle became smaller. The stiffness values at 75°, 60°, and 45° were 173%, 262%, and 406% of that at 90°, respectively. When in the C-S mode, the stiffness of the connection became smaller as the angle decreased from 90° to 75°, and the stiffness of the 75° specimen was 56% of that at 90°. Over the interval of 75° to 45°, the stiffness increased as the angle became smaller. The stiffness values for the 60° and 45° specimens were 134% and 172% of that for the 90° specimen, respectively. The change trend of the stiffness of the test with support was the same as that of the test without support, and the stiffness values at 75°, 60°, and 45° were 75%, 191%, and 219% of that at 90°, respectively.

Calculation Method Analysis for the Load-bearing Capacity

In most of the current practical projects, the calculation according to EC5 is most commonly used. However, the results in Table 3 show that the load-bearing capacity formula of EC5 (EN 1995-1-1 2008) did not fit the inclined screw data well.

Based on a large number of experimental findings, Bejtka and Blaß (2002) analyzed the mechanism of self-tapping screws subjected to a T-S load. Then, they proposed a formula for calculating the load-bearing capacity of inclined screws connected to solid wood based on the European yielding formula in EC5. Later, Tomasi *et al.* (2010) confirmed that the formula could be applied to the calculation of the load-bearing capacity of inclined screws connected to glue-laminated timber.

This study verified whether the formula can be used for the calculation of the bearing capacity of self-tapping screws connecting LVL in the T-S and 90° S modes. According to the formula and combined with this test, Eq. 3 was used to calculate the load-bearing capacity. Geometrical quantities and other terms are explained in Fig. 7. The calculation results are shown in Table 3. This study proposed a load-bearing capacity formula under C-S that was based on the existing formula, and then verified the proposed formula:

$$F_{v,Rk} = F_{ax,Rk} \cdot (\mu \cdot \sin\alpha + \cos\alpha) + (1 - \mu\cot\alpha) \cdot \sqrt{\frac{2 \cdot \beta}{1+\beta}} \sqrt{2 \cdot M_{y,Rk} \cdot f_{h,1,k} \cdot d \cdot \cos^2\alpha} \tag{3}$$

where $F_{\mathrm{v,Rk}}$ is the characteristic load-carrying capacity per shear plane per fastener (N), $f_{\mathrm{h,1,k}}$ is the characteristic embedment strength in the side member (N), d is the fastener diameter (mm), $M_{\mathrm{y,Rk}}$ is the characteristic fastener yield moment (N·mm), β is the ratio between the embedment strength of the members, and $F_{\mathrm{ax,Rk}}$ is the characteristic axial withdrawal capacity of the fastener (N) ($F_{ax,Rk} = min\begin{cases}F_{ax,1,Rk}\\F_{ax,2,Rk}\end{cases}$).

For the C-S (without support) specimen, when there were various angles between the screw axis and grain direction, the load transfer mechanism involved not only the bending capacity of the screw and embedment strength of the wood, but also the withdrawal capacity of the screws. Based on the mechanical model developed by Tomasi *et al*. (2010) (hereafter referred to as Tomasi's model), a model was formed and is shown as Eq. 4,

$$F_{\mathrm{v,Rk}} = \frac{1}{\left[\left(\frac{\cos\alpha}{F_{\mathrm{ax,a,Rk}}}\right)^2 + \left(\frac{\sin\alpha}{V_{\mathrm{y,Rk}}}\right)^2\right]^{1/2}} \tag{4}$$

$$V_{\mathrm{y,Rk}} = V_{\mathrm{adm}} \cdot \pi \cdot \frac{1}{4} d^2 \tag{5}$$

where $F_{\mathrm{v,Rk}}$ and $F_{\mathrm{ax,Rk}}$ are same as that for Eq. 3, $V_{\mathrm{y,Rk}}$ is the shear capacity standard value of the self-tapping screw (N), V_{adm} is the shear strength characteristic value (N), and d is the outer diameter of the self-tapping screw thread (mm).

When the LVL specimen was in the C-S stress mode (with support) and because the lateral support prevented the auxiliary material from slipping outward, the influence of friction on the load-bearing capacity could not be neglected. Tomasi's model does not consider the influence of friction in the C-S mode, so a formula was derived for inclined screws connecting LVL that considered friction and was based on existing formulas. The following proposed model was obtained by fitting the formula. The friction is represented with Eq. 6:

$$F_\mu = \mu \cdot (H_1 + H_2) \tag{6}$$

$$H_1 = F_{ax,1} \cdot \cos\alpha - F_{lat,1} \cdot \sin\alpha \tag{7}$$

$$H_2 = F_{ax,2} \cdot \cos\alpha - F_{lat,2} \cdot \sin\alpha \tag{8}$$

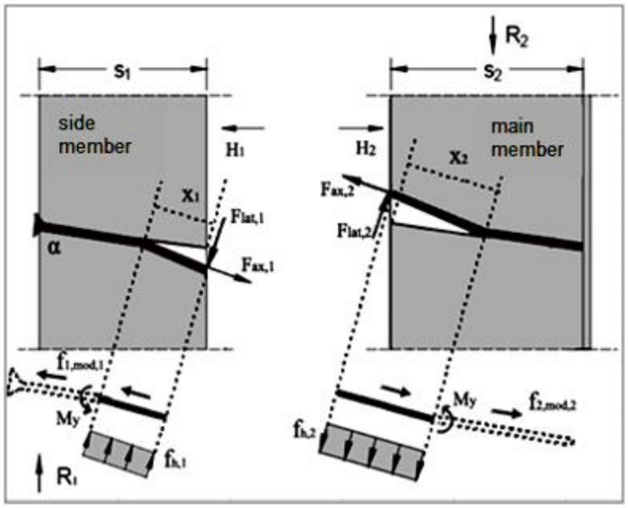

Fig. 7. Analysis diagram of the bearing capacity and stress of the self-tapping screw in the T-S mode

The axial and lateral bearing capacities of the self-tapping screws in the side and main members were determined with the following formulas:

$$F_{lat,1} = \frac{f_{h,1} \cdot d \cdot x_1}{\cos\alpha} \tag{9}$$

$$F_{lat,2} = \frac{f_{h,2} \cdot d \cdot x_2}{\cos\alpha} \tag{10}$$

$$F_{ax,1} = \frac{f_{1,\text{mod},1} \cdot d \cdot s_1}{\cos\alpha} \tag{11}$$

$$F_{ax,2} = \frac{f_{2,\text{mod},2} \cdot d \cdot s_2}{\cos\alpha} \tag{12}$$

The design theory and formula of Bejtka and Blaß (2002) was as follows:

$$X_1 = \sqrt{\frac{2\cdot\beta}{1+\beta}} \cdot \sqrt{\frac{2\cdot M_y \cdot cos\,\alpha^2}{d\cdot f_{h,1}}} \tag{13}$$

$$X_2 = \frac{(\mu + tan\,\alpha)\cdot(f_{1,mod,1}\cdot s_1 - f_{1,mod,2}\cdot s_2)}{\beta\cdot f_{h,1}\cdot(1-\mu\cdot tan\,\alpha)} + \frac{X_1}{\beta} \tag{14}$$

Substituting Eqs. 7 through 14 into Eq. 6 gives:

$$F_\mu = \mu \cdot \left(f_{1,mod,1} \cdot d \cdot s_1 + f_{1,mod,2} \cdot d \cdot s_2 - \frac{f_{h,1}\cdot d\cdot sin\,\alpha}{cos\alpha} \cdot \sqrt{\frac{2\cdot\beta}{1+\beta}} \cdot \sqrt{\frac{2\cdot M_y \cdot sin\,\alpha^2}{d\cdot f_{h,1}}} \right) \tag{15}$$

The load-bearing capacity model of the specimens with support in the C-S mode was as follows,

$$F_{v,Rk} = \frac{1}{\left[\left(\frac{cos\alpha}{F_{ax,a,Rk}}\right)^2 + \left(\frac{sin\,\alpha}{V_{y,Rk}}\right)^2\right]^{\frac{1}{2}}} + \mu \cdot \left(f_{1,mod,1} \cdot d \cdot s_1 + f_{1,mod,2} \cdot d \cdot s_2 - \frac{f_{h,1}\cdot d\cdot sin\alpha}{cos\alpha} \cdot \sqrt{\frac{2\cdot\beta}{1+\beta}} \cdot \sqrt{\frac{2\cdot M_y \cdot sin\alpha^2}{d\cdot f_{h,1}}} \right) \tag{16}$$

where F_{μ} is the friction (N), H_1 and H_2 are combined forces in the horizontal direction, α is the angle of the screw axis and grain direction (°), μ is the friction coefficient at the interface between the wood elements, $F_{ax,1}$ and $F_{ax,2}$ are the axial capacities of the fastener (N), $F_{lat,1}$ and $F_{lat,2}$ are the lateral capacities of the fastener (N), X_1 and X_2 are the distances from the self-tapping screw and plastic hinge to the shearing surface in the side and main members (mm), respectively, $f_{h,1}$ and $f_{h,2}$ are the characteristic embedment strengths of the side and main members (N), respectively, $f_{1,mod,1}$ and $f_{1,mod,2}$ are the withdrawal capacities of the fasteners of the side and main members (N), respectively, M_y is the yield bending moment (N·mm), and S_1 and S_2 are the sizes of the side and main members, respectively.

Figure 8 and Table 4 show that the load-bearing capacity formula in EC5 applied only for the calculation of the bearing capacity of the 90° S and C-S modes without friction. This formula greatly underestimated the bearing capacity of the self-tapping screws in the T-S stress mode, and the safety factor was approximately 1.65 to 1.73. At the same time, it could not be used to calculate the connector with support (friction) in actual engineering.

Table 4. Comparison of the Load-bearing Capacities of the Proposed Model, Test Results, and EC5 (Single Screw)

Configuration	45° T-S	60° T-S	75° T-S	90° S	75° C-S	60° C-S	45° C-S
Test Result (N)	3998 (3943)	4234 (4131)	4126 (4230)	3096 (3057)	2209 (2544)	2233 (3474)	2314 (4198)
EC5 (N)	2312 (2312)	2500 (2500)	2478 (2478)	2476 (2476)	1631 (1631)	1697 (1697)	1753 (1753)
Proposed Model (N)	3161 (3161)	3396 (3396)	2825 (2825)	2245 (2245)	2184 (2475)	2274 (3402)	2417 (4096)
η_1	1.73 (1.68)	1.69 (1.65)	1.67 (1.71)	1.25 (1.23)	1.35 (1.56)	1.23 (2.05)	1.23 (2.39)
η_2	1.26 (1.25)	1.25 (1.22)	1.46 (1.50)	1.38 (1.36)	1.01 (1.03)	0.98 (1.02)	0.96 (1.02)

η_1 is the safety factor calculated by the equation Test Result / EC5; η_2 is the safety factor calculated by the equation Test Result / Proposed Model; the results with support are given in parentheses; the results without support are given without parentheses.

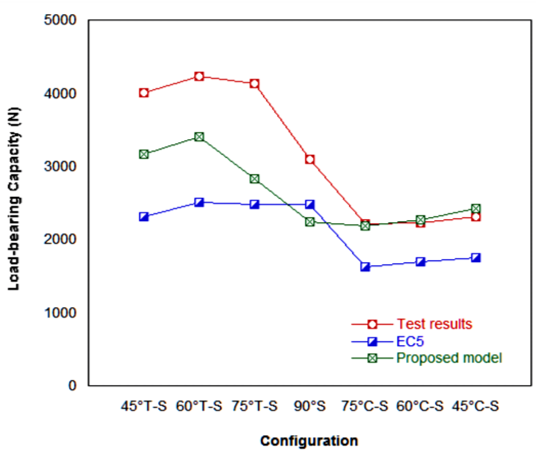

a

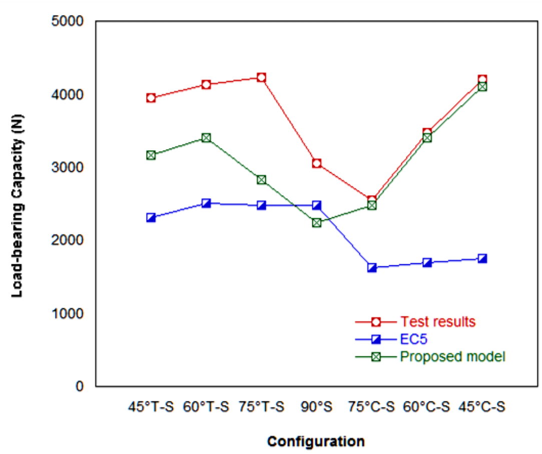

b

Fig. 8. Comparison of the test results with those of EC5 and the proposed formula: without (a) and with support (b)

Figure 9 shows that the proposed model had a high degree of fit with the results in both test sets. At the same time, the proposed formula had the same trend as that of the experimental results for the specimens subjected to the T-S stress mode. In this work a further attempt was made to add a coefficient to the calculation of the specimen subjected to the T-S stress mode and fit the proposed formula with the experimental results. The fitting coefficient (*K*) was 1.25, and the fitting results are shown in Fig. 10.

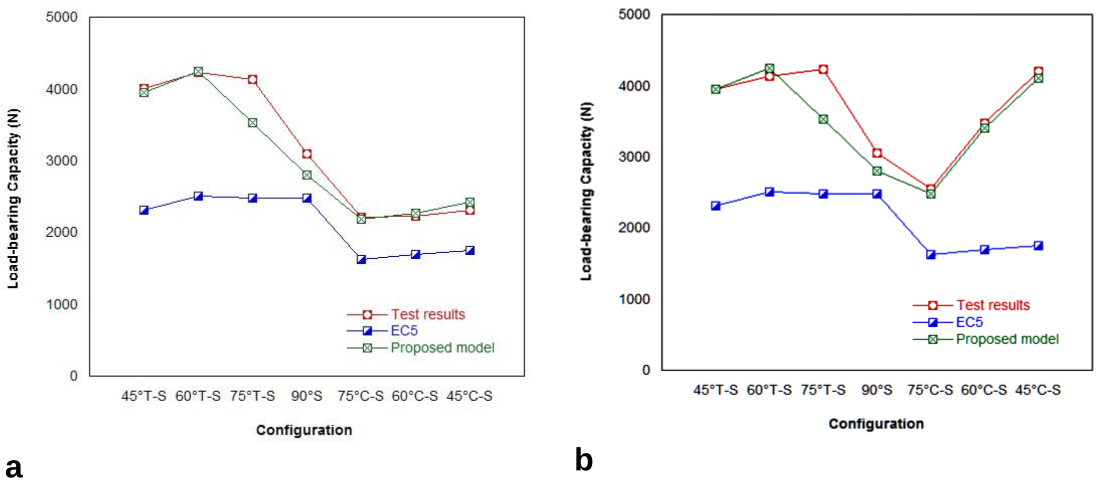

Fig. 9. Comparison of the test results with those of EC5 and the proposed formula after fitting: without (a) and with support (b)

The results of the tests and theoretical calculations demonstrated that the model proposed by Bejtka and Blaß (2002) for self-tapping screws connecting solid wood can better reflect inclined screws connecting LVL in the T-S stress mode after increasing the *K* value to 1.25. The safety factor was approximately 0.97 to 1.19. Tomasi's model for self-tapping screws connecting glue-laminated timber could better reflect inclined screws connecting LVL in the C-S stress mode without support, and the safety factor was approximately 0.96 to 1.01. For actual engineering, the model that this paper proposed for the load-bearing capacity when subjected to the C-S stress mode with support better fit the test results, and the safety factor was approximately 1.02 to 1.03.

Calculation Method Analysis for the Stiffness

The stiffness calculation formula in EC5 does not mention the influence of the angle change on the stiffness. Therefore, regardless of self-tapping screw penetration at any angle, the stiffness calculation results were the same value. The calculation and test results are shown in Table 5.

Table 5 shows that the calculation formula of the stiffness in EC5 was not applicable in all of the C-S modes at 90° S and 75° T-S modes, and it cannot reflect the influence of the angle on the bearing stiffness of self-tapping screws connecting LVL.

Table 5. Comparison of the Stiffness Results of the Test and EC5

Configuration	45° T-S	60° T-S	75° T-S	90° S	75° C-S	60° C-S	45° C-S
Test Results (N)	14588 (15145)	9828 (9375)	6226 (6424)	3814 (3508)	2150 (2888)	5112 (6692)	6570 (7666)
EC5 (N)	7920	7920	7920	7920	7920	7920	7920
$\boldsymbol{\eta_3}$	1.84	1.24	0.78	0.48	0.27	0.65	0.83
$\boldsymbol{\eta_4}$	1.91	1.18	0.81	0.44	0.36	0.84	0.97

The results with support are given in parentheses; the results without support are given without parentheses; η_3 is the safety factor calculated by Results of the test without support / EC5 model; and η_4 is the safety factor calculated by Results of the test with support / EC5 model.

Considering that the current standard and research foundation have not yet established a complete calculation model of the bearing stiffness of inclined screws connecting LVL, the analysis was based on the mechanical model of the self-tapping screw connection of Tomasi *et al.* (2010), whose test results showed that the angle has no effect on the stiffness in the C-S modes. The test results were consistent with those at 90°, which were quite different from the results of inclined screws connecting LVL in this paper.

$$F_{v,Rk} = K_{lat} \cdot \delta \cdot \sin\alpha \cdot (sin\alpha - \mu \cdot cos\alpha) + K_{ax} \cdot \delta \cdot \cos\alpha \cdot (cos\alpha + \mu \cdot sin\alpha) \quad (17)$$

$$F_{\mathrm{v,Rk}} = K_{\mathrm{v,Rk}} \cdot \delta \quad (18)$$

$$K_{v,Rk} = K_{lat} \cdot \sin\alpha \cdot (sin\alpha - \mu \cdot cos\alpha) + K_{ax} \cdot \cos\alpha \cdot (cos\alpha + \mu \cdot sin\alpha) \quad (19)$$

$$K_{\mathrm{lat}} = \frac{K_{\mathrm{test}}}{n_{\mathrm{ef}}} \quad (20)$$

$$K_{\mathrm{ax}} = \frac{1}{\frac{1}{K_{\mathrm{ser,ax,1}}} + \frac{1}{K_{\mathrm{ser,ax,2}}}} \quad (21)$$

$$K_{\mathrm{ser}} = 780 d^{0.2} \cdot l_{\mathrm{ef}}^{0.4} \quad (22)$$

In the above equations, $F_{\mathrm{v,Rk}}$ is the elastic force of each of the shear faces for each connector; K_{lat} is the slip modulus when the self-tapping screw is subjected to a lateral force; δ is the displacement of the self-tapping screw deformation, namely the distance from C1 to C2 (Fig. 10); μ is the friction coefficient of the wood components; K_{test} is the test value of the slip modulus in the 90° test group; n_{ef} is the number of effective screws in the specimens; K_{ax} is the axial slip modulus of the screw; d is the outer thread diameter (mm); l_{ef} is the penetration length in the structural member (mm); and $K_{\mathrm{ser,ax,i}}$ is the axial slip modulus of the threaded part anchored by length l_{i} (mm) in the wood element (Eq. 22 of European Technical Assessment (2016)).

Because there is no definite formula for calculating the stiffness of self-tapping screws connecting LVL, the K_{lat} variable was selected from the test results of the 90° specimens. The lateral support had an almost negligible effect on the self-tapping screws connecting LVL in the T-S and 90° S modes, so the values were the average values of the stiffness of all of the 90° specimens in both test sets. Similarly, the data from this section were the averages of all of the specimens in both test sets in the T-S stress modes.

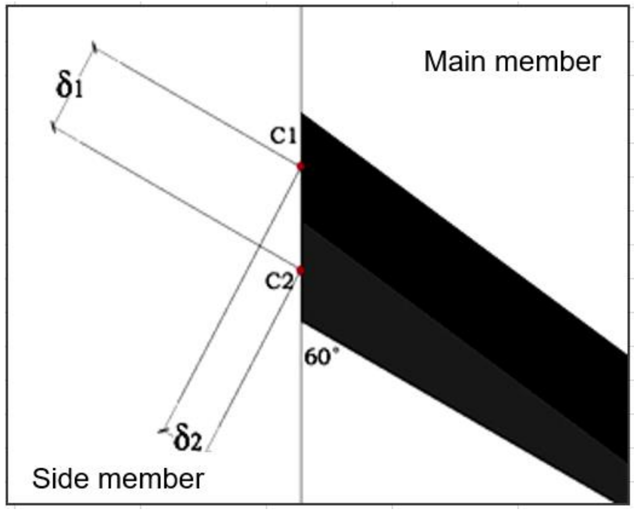

Fig. 10. Schematic diagram of deformation displacement of the self-tapping screw

For screws in the C-S stress test, the mechanical behavior of the screws had proven to be more complex and less efficient. By observing the specimen after failure, it had two steps before failure (Fig. 11). The plastic hinge appeared in the side member first. Then, the component $M_{y,Rk}$ in the main member increased because the angle increased. This led to the second plastic hinge appearing in the main member. These two parts of the screw were lacking in synergy. A penalty value of φ was needed. In this test, by fitting the formula, φ was 0.5. When there was no lateral support, the friction no longer existed and Eq. 22 was obtained. However, when the lateral support was arranged and considering the existence of friction, Eq. 23 was obtained.

$$K_{\mathrm{v,Rk}} = K_{\mathrm{lat}}\sin\alpha^2 + K_{\mathrm{ax}}\cos\alpha^2 \tag{22}$$

$$K_{v,Rk} = K_{lat} \cdot \sin\alpha \cdot (sin\alpha + \mu \cdot cos\alpha) + K_{ax} \cdot \cos\alpha \cdot (cos\alpha + \mu \cdot sin\alpha) \tag{23}$$

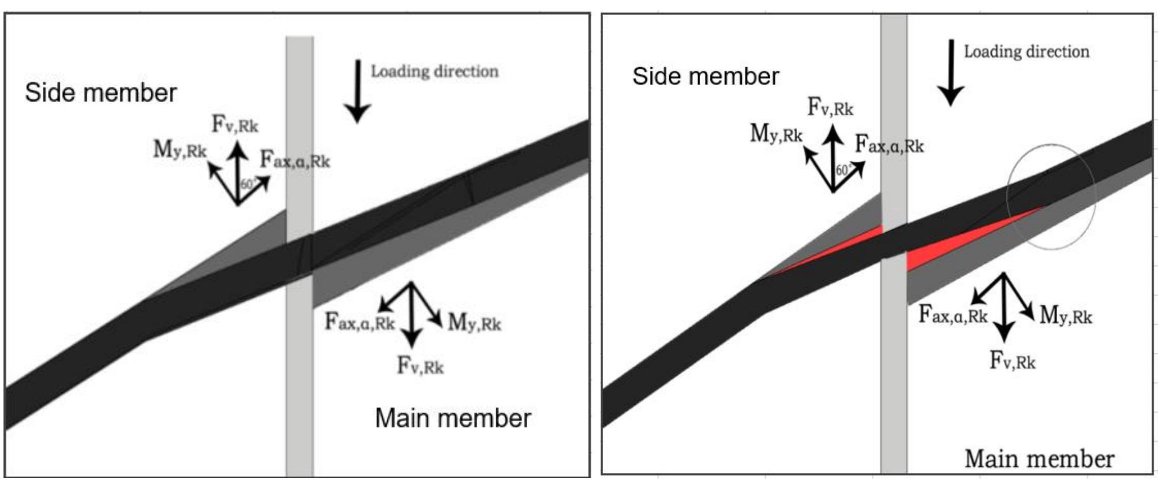

Fig. 11. Model of the two steps of the plastic hinge

Table 6. Comparison of the Stiffness of Tomasi's Model and Proposed Model Test Results (Single Screw)

SP	45° T-S	60° T-S	75° T-S	90° S	75° C-S	60° C-S	45° C-S
Test Results (N/mm)	4252 (4352)	2774 (2694)	1819 (1846)	1049 (1049)	618 (830)	1469 (1923)	1888 (2203)
Proposed Model (N/mm)	3754 (3754)	2866 (2866)	1706 (1706)	1049 (1049)	1150 (1375)	1424 (1813)	1764 (2205)
Tomasi's Model (N/mm)	1943	1586	1244	1049	1049	1049	1049
η_5	1.13	0.97	1.07	1	0.54	1.03	1.07
η_6	1.16	0.94	1.08	1	0.61	1.06	1.00

The results with support are given in parentheses; the results without support are given without parentheses; η_5 is the safety factor calculated by Results of the tests without support / Proposed model without support; and η_6 is the safety factor calculated by Results of the tests with support / Proposed model with support.

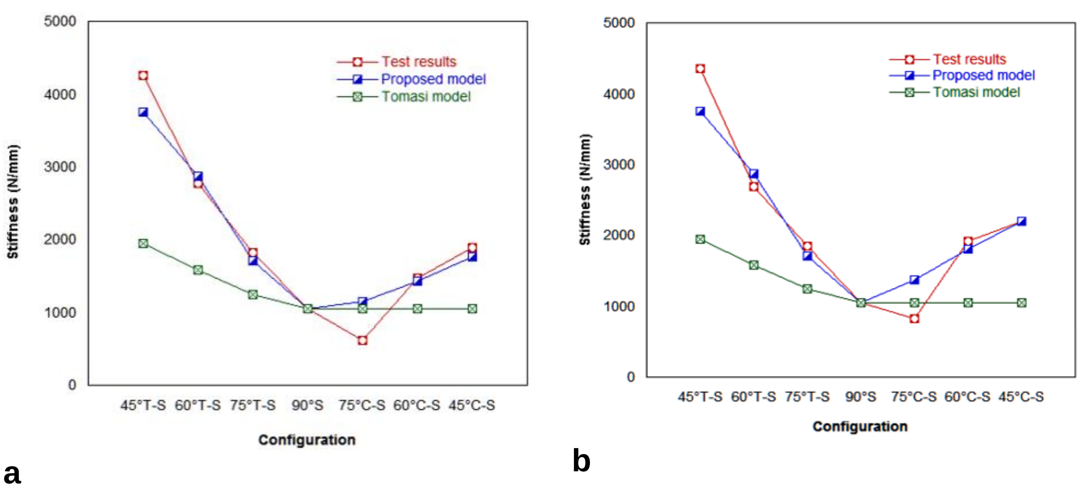

Fig. 12. Comparison of the stiffness from Tomasi's model, the proposed model, and test results: without (a) and with support (b)

Table 6 and Fig. 12 show that the proposed model for calculating the stiffness of the inclined screw connecting the LVL was well fitted to the test results when the joint was subjected to the T-S force mode, and 60° and 45° C-S force modes. The safety factor was approximately 0.97 to 1.13. However, the calculation results of the proposed formula differed greatly from the test results from the 75° C-S stress mode.

CONCLUSIONS

1. Compared with the 90° screw connection, the inclined screw had a higher shear bearing capacity, and the inclined screw with an angle of 45° to 60° had a higher bearing capacity than at the other angles. The load-bearing capacity and bearing stiffness in the T-S mode were better than in the C-S mode. The lateral support increased the load-bearing capacity and stiffness of the C-S force mode, but it had little effect on the

bearing capacity and bearing stiffness in the T-S stress mode. The 75° pressure-shear was demonstrated to be an inefficient connection method. It is recommended to use a 45° to 60° screw angle connection.

2. The theoretical formula from Bejtka and Blaß (2002) for self-tapping screws connecting solid wood better reflected the bearing capacity of inclined screws connecting LVL in the T-S stress mode after increasing the K to 1.25. The safety factor was approximately 0.97 to 1.19. Tomasi's model for self-tapping screws connecting glue-laminated timber better reflected the bearing capacity of inclined screws connecting LVL in the C-S stress mode without support, and the safety factor was approximately 0.96 to 1.01. In actual engineering, when subjected to the C-S stress mode under the support of both sides of the connecting member, the model proposed in this paper better fit the test results, and the safety factor was approximately 1.02 to 1.03.
3. The EC5 stiffness calculation formula and Tomasi's stiffness calculation formula cannot be used for inclined screws connecting LVL. The formula proposed in this paper for calculating the bearing stiffness of inclined screws connecting LVL was fit to the test results in the T-S mode, and 60° and 45° C-S modes. The safety factor was approximately 0.97 to 1.13. However, the calculation results of the proposed model differed greatly from the test results from the 75° C-S mode.

ACKNOWLEDGMENTS

This work was supported by the National Natural Science Foundation of China (Grant No. 31670566).

REFERENCES CITED

Adachi, K., Yamauchi, H., Kojima, K., and Inoue, M. (2010). "Improvement in flexibility of laminated veneer lumber by using pressure-sensitive adhesives," in: *World Conference 15 on Timber Engineering*, Trentino, Italy.

Audebert, M., Dhima, D., Taazount, M., Bouchaïr, A. (2012). "Behavior of dowelled and bolted steel-to-timber connections exposed to fire," *Engineering Structures* 39, 116-125. DOI: 10.1016/j.engstruct.2012.02.010

Bal, B. C., and Bektaş, I. (2012). "The effects of some factors on the impact bending strength of laminated veneer lumber," *BioResources* 7(4), 5855-5863. DOI: 10.15376/biores.7.4.5855-5863

Bal, B. C. (2014). "Flexural properties, bonding performance and splitting strength of LVL reinforced with woven glass fiber," *Constr. Build. Mater.* 51, 9-14. DOI: 10.1016/j.conbuildmat.2013.10.041

Bal, B. C., Özdemir, F., and Altuntaş, E. (2013). "A comparative study on screw withdrawal strength of solid wood material and laminated veneer lumber," *Ormancılık Dergis* 9(2), 14-22.

Bejtka, I., and Blaß, H. J. (2002). "Joints with inclined screws," in: *Proceedings from Meeting Thirty-five of the International Council for Building Research Studies and Documentation, CIB, Working Commission W18 – Timber Structure*, Kyoto, Japan.

Burdurlu, E., Kılıç, M., Ilçe, A. C., and Uzunkavak, O. (2007). "The effects of ply organization and loading direction on bending strength and modulus of elasticity in laminated veneer lumber (LVL) obtained from beech (*Fagus orientalis* L.) and lombardy poplar (*Populus nigra* L.)," *Constr. Build. Mater.* 21(8), 1720-1725, DOI: 10.1016/j.conbuildmat.2005.05.002.

Celebi, G., and Kilic, M. (2007). "Nail and screw withdrawal strength of laminated veneer lumber made up hardwood and softwood layers," *Constr. Build. Mater.* 21(4), 894–900. DOI: 10.1016/j.conbuildmat.2005.12.015

EN 1995-1-1 (2008). "Eurocode 5: Design of timber structures – Part 1-1: General. Common rules and rules for buildings," European Committee for Standardization, Brussels, Belgium.

EN 12512:2001 (2001). "Timber structures – Test methods – Cyclic testing of joints made with mechanical fasteners," European Committee for Standardization, Brussels, Belgium.

EN 26891:1991 (1991). "Timber structures. Joints made with mechanical fasteners – General principles for the determination of strength and deformation characteristics," European Committee for Standardization, Brussels, Belgium.

Ellingsbo, P., and Malo, K. A. (2012). "Withdrawal capacity of long self-tapping screws parallel to grain direction," World Conference on Timber Engineering, Auckland, Nao Zealand.

ETA-11/0030 (2016). "European Technical Assessment," European Organization for Technical Assessment (EOTA).

Gaff, M., and Gašparík, M. (2015). "Influence of densification on bending strength of laminated beech wood," *BioResources* 10(1), 1506-1518. DOI: 10.15376/biores.10.1.1506-1518

Hossain, A., Lakshman, R., and Tannert, T. (2015). "Shear connections with self-tapping-screws for cross-laminated-timber panels," in: *Proceedings of Structures Congress*, Portland, OR.

Johansen, W. K. (1949). "Theory of timber connections," *International Association of Bridge and Structural Engineering* 9, 249-262. DOI: 10.5169/seals-9703

Kılıç, M. (2011). "The effects of the force loading direction on bending strength and modulus of elasticity in laminated veneer lumber (LVL)," *BioResources* 6(3), 2805-2817. DOI: 10.15376/biores.6.3.2805-2817

LY/T 2377-2014 (2014). "Test methods for the joint performance with dowel type fasteners used in wooden structural material," State Forestry Administration, Beijing, China.

Ozarska, B. (1999). "A review of the utilisation of hardwoods for LVL," *Wood Sci. Technol.* 33(4), 341-351. DOI: 10.1007/s002260050120

Özçifçi, A. (2009). "The effects of pilot hole, screw types and layer thickness on the withdrawal strength of screws in laminated veneer lumber," *Mater. Design* 30(7), 2355-2358. DOI: 10.1016/j.matdes.2008.11.001

Shukla, S. R., and Kamdem, D. P. (2008). "Properties of laminated veneer lumber (LVL) made with low density hardwood species: Effect of the pressure duration," *Holz Roh. Werkst.* 66(2), 119-127. DOI: 10.1007/s00107-007-0209-1

Shukla, S. R., and Kamdem, D. P. (2009). "Properties of laboratory made yellow poplar (*Liriodendron tulipifera*) laminated veneer lumber: Effect of the adhesives," *Eur. J. Wood Wood Prod.* 67(4), 397-405. DOI: 10.1007/s00107-009-0333-1

Sulaiman, O., Salim, N., Hashim, R., Yusof, L. H. M., Razak, W., Yunus, N. Y. M., Hashim, W. S., and Azmy, M. H. (2009). "Evaluation on the suitability of some adhesives for laminated veneer lumber from oil palm trunks," *Mater. Design* 30(9), 3572–3580. DOI: 10.1016/j.matdes.2009.02.027

Tomasi, R., Crosatti, A., and Piazza, M. (2010). "Theoretical and experimental analysis of timber-to-timber joints connected with inclined screws," *Constr. Build. Mater.* 24(9), 1560-1571. DOI: 10.1016/j.conbuildmat.2010.03.007

Wang, B. J., and Dai, C. (2005). "Hot-pressing stress graded aspen veneer for laminated veneer lumber (LVL)," *Holzforschung* 59(1), 10-17. DOI: 10.1515/HF.2005.002

Zhang, X. L., Que, Y. L., Wang, X. M., Li, Z. R., Zhang, L. L., Han, C., Que, Z. L., and Komatsu, K. (2018). "Experimental behavior of laminated veneer lumber with round holes, with and without reinforcement," *BioResources* 13(4), 8899-8910. DOI:10.15376/biores.13.4.8899-8910

Article submitted: October 14, 2018; Peer review completed: January 19, 2019; Revised version received: March 24, 2019; Accepted: March 25, 2019; Published: March 29, 2019.
DOI: 10.15376/biores.14.2.4006-4021